

Proceedings Article

# A Dictionary-Based Algorithm for MNP Signal Prediction at Unmeasured Drive Field Frequencies

Asli Alpman <sup>a,b,\*</sup>. Mustafa Utkur <sup>a,b,c,d</sup>. Emine Ulku Saritas <sup>a,b,e</sup>

<sup>a</sup>Department of Electrical and Electronics Engineering, Bilkent University, Ankara, Turkey

<sup>b</sup>National Magnetic Resonance Research Center (UMRAM), Bilkent University, Ankara, Turkey

<sup>c</sup>Harvard Medical School, Boston, MA, United States

<sup>d</sup>Boston Children's Hospital, Boston, MA, United States

<sup>e</sup>Neuroscience Program, Sabuncu Brain Research Center, Bilkent University, Ankara, Turkey

\*Corresponding author, email: [alpman@ee.bilkent.edu.tr](mailto:alpman@ee.bilkent.edu.tr)

© 2023 Alpman *et al.*; licensee Infinite Science Publishing GmbH

This is an Open Access article distributed under the terms of the Creative Commons Attribution License (<http://creativecommons.org/licenses/by/4.0>), which permits unrestricted use, distribution, and reproduction in any medium, provided the original work is properly cited.

## Abstract

The signal in MPI depends on magnetic nanoparticle (MNP) parameters and environmental conditions, as well as drive field (DF) settings and measurement system response. In this study, we propose a dictionary-based algorithm using a coupled Brown-Néel rotation model to simultaneously estimate the MNP parameters together with system transfer function. We then propose an empirical method that enables signal prediction at unmeasured DF frequencies, where measurement data is not available.

## I. Introduction

Magnetic Particle Imaging (MPI) utilizes the nonlinear magnetization response of magnetic nanoparticles (MNPs), governed by two main mechanisms: Néel and Brownian rotation. In the Brownian process, MNP physically rotates to align its magnetic moment with the applied field, whereas the Néel process internally flips the magnetic moment [1]. The Brownian and Néel mechanisms are coupled such that the physical rotation of the MNP and the magnetic moment rotation are interdependent.

Previous work has shown that applications of MPI, such as relaxation-based viscosity mapping and temperature mapping, may have optimal drive field (DF) frequencies that are different than the commonly used 25 kHz [2, 3]. However, determining the optimal DF settings requires extensive experimental measurements. To better understand the trends in the MNP response, accurate

modeling of the underlying physics is crucial. Previous work employed model-based simulation approaches to explain the magnetic response and estimate the parameters of MNPs [4–6].

In this work, we propose a dictionary-based method that also accounts for measurement system response to estimate the parameters that give rise to the measured MNP signal. We also propose an empirical method to predict the system response at DF frequencies where no measurement data is available, enabling MNP signal prediction unmeasured DF frequencies.

## II. Methods and Materials

### II.1. Dictionary Preparation

The magnetization responses of MNPs with varying magnetic parameters under sinusoidal DFs were simulated

by solving ordinary differential equations given in [7], derived from the Fokker-Planck equations of a coupled Brown-Néel rotation model. The simulated MNPs had uniaxial magnetic anisotropy constant ( $K$ ) ranging from  $1 \text{ kJ m}^{-3}$  to  $10 \text{ kJ m}^{-3}$ , core diameter ( $d_c$ ) ranging from 5 nm to 30 nm, and hydrodynamic diameter ( $d_h$ ) ranging from 20 nm to 130 nm. In total, the responses for 4680 different MNPs were simulated. The response of each MNP was simulated at 6 different DFs with 10 mT and 15 mT amplitude and 250 Hz, 1 kHz, and 2 kHz frequency. These relatively low frequencies were chosen, as they were previously shown to have high viscosity sensitivity [3, 8]. In addition, the simulations were repeated at 6 different viscosity levels ( $\eta$ ) ranging from  $0.893 \text{ mPa} \cdot \text{s}$  to  $15.33 \text{ mPa} \cdot \text{s}$ . The Gilbert damping constant, saturation magnetization, and temperature were assumed to be 0.1, 360 kA/m, and  $25^\circ\text{C}$ , respectively. At the considered frequencies, the coupled Brown-Neel rotation model provided considerably different MNP signals than the simpler Brown-only and Langevin models, underscoring the importance of accurate modeling.

## II.II. Problem Formulation

Assuming that the measurement setup can be modeled as a linear time-invariant (LTI) system, we formulated the problem in the frequency domain to solve simultaneously for the transfer function (TF) of the measurement setup and the dictionary weights. Note that the TFs vary with the DF settings, since both the transmit and receive chain characteristics change with the applied DF amplitude and frequency. While the estimated weights enable us to estimate the magnetic parameters of the tested MNP, the estimated TF allows us to characterize the system in a calibration-free manner. We formulate this problem as follows:

$$\min_{x \in \mathbb{R}^{n \times 1}, H \in \mathbb{R}^{m \times m}} \|H Ax - b\|_2^2 \quad \text{s.t.} \quad x \geq 0 \quad (1)$$

where  $A \in \mathbb{R}^{m \times n}$  is the dictionary matrix constructed with the simulated MNP signals,  $b \in \mathbb{R}^{m \times 1}$  is the measurement vector with concatenated experimental data from different viscosity levels,  $H \in \mathbb{R}^{m \times m}$  is the diagonal matrix with the TF values as diagonal entries,  $n$  is the number of MNPs in the dictionary,  $m$  is the total number of harmonics used for parameter estimation, and  $x \in \mathbb{R}^{n \times 1}$  is the vector of dictionary weights. To integrate different DFs into the problem, we concatenated the corresponding matrices from the different DFs vertically. Then, we simultaneously solved for  $H$  and a common optimal  $x$  using alternating minimization methods, i.e., keeping one variable fixed while the other variable is optimized.

It should be noted that there are infinitely many  $(x, H)$  pairs that satisfy Eq. 1 but have different scalings, i.e.,  $(kx, H/k)$  for some arbitrary constant  $k$ . However, such a scaling does not affect the MNP signal prediction re-

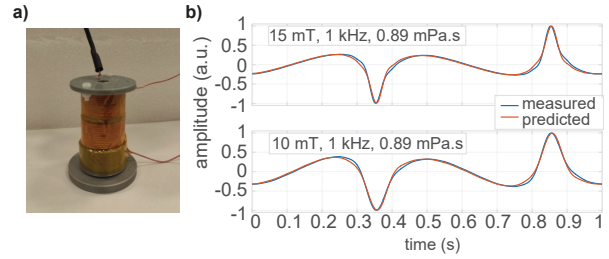


**Figure 1:** (a) In-house arbitrary waveform MPS setup. (b) Example measured and predicted signals (normalized together) for the sample at  $0.89 \text{ mPa} \cdot \text{s}$  viscosity level, at two different field amplitudes at 1 kHz DF frequency.

sults since  $x$  and  $H$  are eventually multiplied for signal prediction purposes.

## II.III. Transfer Function and Signal Prediction

Unless we have measured data at a specific DF, the TF for that DF can not be obtained via Eq 1. For this purpose, we propose an empirical method that predicts the TF at an unmeasured DF frequency and amplitude using the previously estimated TFs at measured DF frequencies with the same amplitude. Accordingly, at each harmonic number, a linear fit is performed to the estimated TF amplitude in logarithmic scale versus the DF frequency in logarithmic scale at the measured DFs. The TF amplitude at the unmeasured DF is then predicted using this linear fit.

For the MNP signal prediction at the unmeasured DF, first a response is simulated considering the dictionary weights. The predicted TF amplitude is then applied to this response to predict the MNP signal.

## II.IV. Quantitative Assessments

Note that we only predict the amplitude of the TF, while directly assigning zero phase to each harmonic to simplify the problem. Since we observed a linear phase response for the TF solutions, ignoring the phase of the TF causes the predicted signal to only be shifted in time. Therefore, a time shift is applied to the predicted signal to quantitatively compare its accuracy with respect to the reference signal (i.e., the actual measured signal at that DF setting). As a quantitative evaluation metric, normalized root mean square error (NRMSE) between the measured and predicted signals was utilized. As a second metric, we compared the normalized root mean square (RMS) amplitudes of the signals as follows:

$$\hat{s}_{rms} = \frac{1}{f_d(Hz) \cdot B_d(T) \cdot Fe(g)} \times \sqrt{\frac{1}{N} \sum_{n=1}^N s_n^2} \quad (2)$$

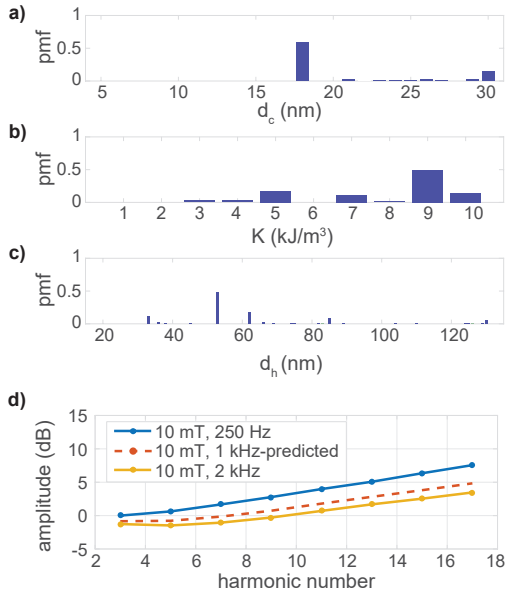


**Figure 2:** MNP parameter and TF estimation results when 1 kHz DF measurements are left out. The probability mass functions for (a)  $d_c$ , (b)  $K$ , and (c)  $d_h$  are displayed. (d) Estimated TF amplitude at 250 Hz and 2 kHz, at 10 mT amplitude. TF amplitudes were normalized with respect to the TF value at the third harmonic of 250 Hz. Dashed line shows the predicted TF amplitude at 1 kHz.

Here, the RMS signal is normalized by DF frequency  $f_d$ , DF amplitude  $B_d$ , and iron content  $Fe$ . Lastly, we compared the time interval between two zero crossing time points in a one-half cycle,  $t_{zc}$ . To enable comparison relative to DF period  $T_d$ , we defined percentage zero-crossing time interval as:

$$\hat{t}_{zc} = \frac{t_{zc}}{T_d} \times 100 \quad (3)$$

## II.V. Experiments

The experiments were performed on an in-house arbitrary waveform magnetic particle spectrometer (MPS) setup, shown in Fig. 1a. The power amplifier (AE Techron 7224) amplifies the DF waveform from the data acquisition card (NI USB-6383) and sends it to the DF coil. The received signal is amplified by a low-noise amplifier (SRS SR560) and sent to a PC to be processed in MATLAB. The experiments were conducted at 10 mT and 15 mT DF amplitudes, at 250 Hz, 1 kHz, and 2 kHz DF frequencies. MNP samples at 6 different viscosity levels were prepared using glycerol and deionized water [9], with each sample containing 26.2  $\mu$ l of Perimag nanoparticles (Micromod GmbH, Germany) with a total volume of 70  $\mu$ l.

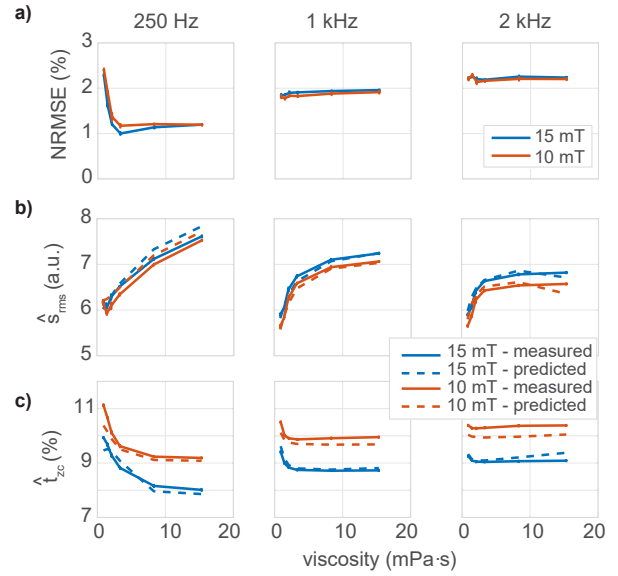


**Figure 3:** Signal prediction accuracy at 3 DF frequencies and 2 DF amplitudes, plotted as a function of sample viscosity. (a) NRMSE of prediction, and (b)  $\hat{s}_{rms}$  and (c)  $\hat{t}_{zc}$  for the predicted and measured signals. In each case, measurements at the relevant DF frequency were entirely left out during prediction.

## III. Results and Discussion

Figure 1b shows the predicted and measured signals at 1 kHz for 0.89 mPa  $\cdot$  s viscosity level. The signal predictions works accurately throughout the period, with the exception of slight mismatches in the signal tails. Figure 2 shows the estimated MNP parameter distribution and the TF amplitudes for the case where 1 kHz DF measurements are left out, together with the predicted TF amplitude at 1 kHz. We observed that the estimated parameter distribution varies only slightly depending on the left out DF frequency. For example, the mean core diameters were 19.9 nm, 21.1 nm, and 20.9 nm for the left out frequencies 250 Hz, 1 kHz, and 2 kHz, respectively.

Figure 3 shows the quantitative assessment results for the prediction. For each case, measurements at the relevant DF frequency were entirely left out during parameter estimation and signal prediction. The predicted response was then compared with the actual measured response at that DF setting. Overall, the signal prediction works successfully at a wide range of DF settings. Accordingly, NRMSE for the signal prediction remains below 3% at all viscosity levels and DF settings. Evaluations on  $\hat{s}_{rms}$  and  $\hat{t}_{zc}$  also demonstrate a close match between the measured and predicted signals, but also provide a better insight regarding the differences between the measured and predicted signals. To illustrate, while NRMSE remains near constant at all viscosity levels at 2 kHz, both  $\hat{s}_{rms}$  and  $\hat{t}_{zc}$  demonstrate a slight deviation between the measured and predicted signals at the highest viscosity.

In this work, we modeled MNPs as single core spheri-

cal particles with uniaxial magnetic anisotropy. Therefore, the estimated distributions in Fig. 2a-c are for “effective parameters” that may not have a full physical correspondence, especially in the case of multicore MNPs. Nonetheless, the quantitative assessments in Fig. 3 demonstrate that these effective parameters successfully capture the trends in MNP signal at different DF settings. Overall, the results indicate that the proposed method works successfully in predicting TFs and MNP signals. Further verification of the proposed method at a wider range of DF settings remains as future work.

## IV. Conclusion

This work proposes an algorithm to predict MNP signals at DF frequencies where no measurement is available, using a model-based dictionary approach. The qualitative and quantitative assessments demonstrate successful signal prediction at unmeasured DF frequencies. The proposed signal prediction approach has potential applications, such as determining the optimal settings for viscosity mapping and temperature mapping using MPI.

## Acknowledgments

This work was supported by the Scientific and Technological Research Council of Turkey (TUBITAK 120E208).

## Author’s statement

Conflict of interest: Authors state no conflict of interest.

## References

- [1] C. Shasha and K. Krishnan. Nonequilibrium dynamics of magnetic nanoparticles with applications in biomedicine. *Advanced Materials*, 33:1904131, 2020, doi:[10.1002/adma.201904131](https://doi.org/10.1002/adma.201904131).
- [2] M. Utkur, Y. Muslu, and E. U. Saritas. Relaxation-based color magnetic particle imaging for viscosity mapping. *Applied Physics Letters*, 115(15):152403, 2019.
- [3] M. Utkur and E. U. Saritas. Simultaneous temperature and viscosity estimation capability via magnetic nanoparticle relaxation. *Medical Physics*, 49(4):2590–2601, 2022.
- [4] A. Neumann, S. Draack, F. Ludwig, and T. M. Buzug. Parameter estimations of magnetic particles: A comparison between measurements and simulations, in *International Workshop on Magnetic Particle Imaging*, 79, 2019.
- [5] H. Albers, T. Kluth, and T. Knopp. Simulating magnetization dynamics of large ensembles of single domain nanoparticles: Numerical study of Brown/Néel dynamics and parameter identification problems in magnetic particle imaging. *Journal of Magnetism and Magnetic Materials*, 541:168508, 2022, doi:<https://doi.org/10.1016/j.jmmm.2021.168508>.
- [6] A. Alpman, M. Utkur, and E. U. Saritas. MNP characterization and signal prediction using a model-based dictionary, in *International Workshop on Magnetic Particle Imaging*, 8, 2022. doi:[10.18416/IJMPI.2022.2203017](https://doi.org/10.18416/IJMPI.2022.2203017).
- [7] J. Weizenecker. The Fokker–Planck equation for coupled Brown–Néel-rotation. *Physics in Medicine & Biology*, 63(3):035004, 2018, doi:[10.1088/1361-6560/aaa186](https://doi.org/10.1088/1361-6560/aaa186).
- [8] M. Utkur, Y. Muslu, and E. U. Saritas. Relaxation-based viscosity mapping for magnetic particle imaging. *Physics in Medicine & Biology*, 62(9):3422, 2017.
- [9] N.-S. Cheng. Formula for the viscosity of glycerol water mixture. *Industrial Engineering Chemistry Research*, 47(9):3285–3288, 2008, doi:[10.1021/ie071349z](https://doi.org/10.1021/ie071349z).